Surface Morphology of PECVD Fluorocarbon Thin Films from Hexafluoropropylene Oxide, 1,1,2,2-Tetrafluoroethane, and Difluoromethane

CATHERINE B. LABELLE, KAREN K. GLEASON

Department of Chemical Engineering, Massachusetts Institute of Technology, Cambridge, Massachusetts 02139

Received 19 March 1998; accepted 13 May 1999

ABSTRACT: Atomic force microscopy (AFM) measurements have been made on a series of fluorocarbon films deposited from pulsed plasmas of hexafluoropropylene oxide (HFPO), 1,1,2,2-tetrafluoroethane ($C_2H_2F_4$), and difluoromethane (CH_2F_2). All of the films give images showing nodular growth (cauliflower-like appearance), with the size and distribution of the nodules dependent on both the precursor, the degree of surface modification to which the growing film is exposed, and the substrate surface. Films deposited from $C_2H_2F_4$ showed clusters of smaller nodules around larger nodules, whereas films deposited from CH_2F_2 were characterized by a uniform distribution of smaller nodules, and films deposited from HFPO had the largest observed nodules. Movchan and Demchishin's structure zone model was applied to the observed films, which were all found to be zone 1 structures, indicating that film growth is dominated by shadowing effects. Increased substrate temperature and incident power per nm of film deposited results in decreased rms roughness, consistent with greater atomic mobility during deposition. Larger nodules in the fluorocarbon films developed on silicon wafer substrates than on rougher Al-coated substrates. Advancing contact angles for all of the films were found to be higher than that of PTFE (108°), indicating both hydrophobic and rough surfaces. Specifically, contact angles of films deposited from HFPO were found to increase with pulse off-time, the same trend observed for both the CF_2 fraction of the film and the rms roughness. © 1999 John Wiley & Sons, Inc. J Appl Polym Sci 74: 2439–2447, 1999

Key words: AFM; PECVD; contact angles; fluorocarbon

INTRODUCTION

Fluorocarbon thin films are currently under investigation for a variety of applications, including biomaterials and semiconductor dielectrics.[1–4] All of these applications would benefit from analysis of the deposited films' surface structure and morphology. Surface morphology influences parameters such as wettability and adhesion, and can affect both the conformality of a particular coating and its etching characteristics (i.e., preferential etching in a particular direction).

Atomic force microscopy (AFM) has been used extensively to study the surfaces of polymers, plasma-deposited polymers, and plasma-modified polymers.[5–13] AFM is especially suited to polymer analysis due to the low applied forces in contact mode, which can be further reduced by using tapping mode. These low forces allow the film surface to be imaged without modification by the force of the AFM tip on the surface.[14] The surfaces of bulk

Correspondence to: K. Gleason.
Contract grant sponsors: Office of Naval Research; Lucent Technologies Bell Laboratories Graduate Research Program for Women; NSF/SRC Engineering Research Center for Environmentally Benign Semiconductor Manufacturing.

Journal of Applied Polymer Science, Vol. 74, 2439–2447 (1999)
© 1999 John Wiley & Sons, Inc. CCC 0021-8995/99/102439-09

polymers including poly(tetrafluoroethylene), polypropylene, polysulfone, and polyimides, as well as organic thin films grown by a variety of deposition techniques, have been studied using AFM.[5,7,9–11,13]

This study focuses on fluorocarbon films deposited using a pulsed-modulated radio frequency plasma (pulsed-plasma enhanced chemical vapor deposition, pulsed-PECVD). Recent work with pulsed fluorocarbon plasmas has shown that significant compositional control can be achieved for deposition from some precursors, and in all cases, the role of the precursor chemistry is significantly more important than for continuous plasma PECVD.[15–17] The range of fluorocarbon film compositions achieved through pulse modulation leads to a range of film material properties, resulting in the possibility of a range of surface morphologies and surface properties.

AFM measurements have been made on films deposited from pulsed plasmas of hexafluoropropylene oxide (HFPO), 1,1,2,2-tetrafluoroethane ($C_2H_2F_4$), and difluoromethane (CH_2F_2). Roughness analyses have been performed on the resulting data, and the effect of the pulse modulation on the surface features has been explored. Contact angle measurements have also been performed to test the wettability of the fluorocarbon films as a function of both deposition precursor and the pulse conditions.

EXPERIMENTAL

Pulsed PECVD films were deposited on both silicon (Si) and sputtered aluminum-coated (~1000 Å) Si wafers. The pulse on-time was either 10 or 40 ms, and the pulse off-time was in the range between 20 and 400 ms. For the gases (DuPont, Wilmington, DE), a flow rate of 12.5 sccm was used for 1,1,2,2-$C_2H_2F_4$ and CH_2F_2, whereas 23 sccm was used for HFPO, all with a peak rf power of 2.7 W/cm^2 at 1000 mPa in a parallel plate reactor. Previous work shows that changing the HFPO flow rate from 12.5 to 23 sccm has little impact on film deposition rate and composition.[15] The wafers were cooled on the backside with water at approximately 23°C.

Atomic force microscopy was used to determine surface roughness, the height of surface features, and the overall appearance of the surface. AFM (Digital Instruments Dimension 3000, Santa Barbara, CA) was used in tapping mode with a standard etched silicon tip to study 2×2 μm areas on the surface of each film. Tapping mode was employed in order to prevent possible surface damage due to continuous contact of the tip with the surface.

Advancing contact angles were measured on static drops of water using a Ramé–Hart manual goniometer (Ramé–Hart, Inc., Mountain Lakes, NJ) equipped with video camera and computer monitor for viewing the drops. Contacting liquids were advanced and retreated (1 μL/s) prior to measurement with a Micro-Electrapette syringe (Matrix Technologies, Lowell, MA). The pipet tip remained in the drop during measurement. Measurements of the approximately 5-μL drops were taken at five different locations on a sample.

RESULTS AND DISCUSSION

Figure 1 shows two-dimensional (2D)AFM surface images of 10 ms on/100 ms off (10/100) pulsed plasma films from $C_2H_2F_4$, CH_2F_2, and HFPO. The three films are of comparable thickness: 516, 364, and 438 nm for the $C_2H_2F_4$, CH_2F_2, and HFPO precursors, respectively. All three films show growth of spherical nodules, with the height and diameter of the nodules dependent on the precursor. Table I lists the deposition conditions, root mean square roughness (R_{rms}), maximum feature height, and nodule diameters (d) for all of the films discussed in this work.

Growth from $C_2H_2F_4$ [Fig. 1(a)] displays clusters of nodules, where smaller nodules ($d \sim 20$–50 nm) group around larger nodules ($d \sim 100$–150 nm), often referred to as a cauliflower-like appearance.[18] The larger nodules may have formed through agglomeration of several smaller nodules over the deposition period. Alternatively, the larger nodules could result from initial growth from a nucleation site on the silicon surface, with subsequent nucleation of additional nodules from the larger one, thus producing arrays of smaller nodules on the larger ones. The maximum feature height is approximately 167 nm, which is nearly 33% of the total 516-nm film, and a large rms surface roughness (R_{rms}) is also seen (22.3 nm).

Deposition from CH_2F_2 [Fig. 1(b)] rather than $C_2H_2F_4$ [Fig. 1(a)] results in smaller nodules of $d \sim 30$–100 nm, distributed uniformly over the scanned area. The nodules are also shorter, with a maximum feature height of approximately 84 nm. This change is reflected in the R_{rms}, which is 11.8 nm, approximately half the R_{rms} observed for the film deposited from $C_2H_2F_4$. The AFM image

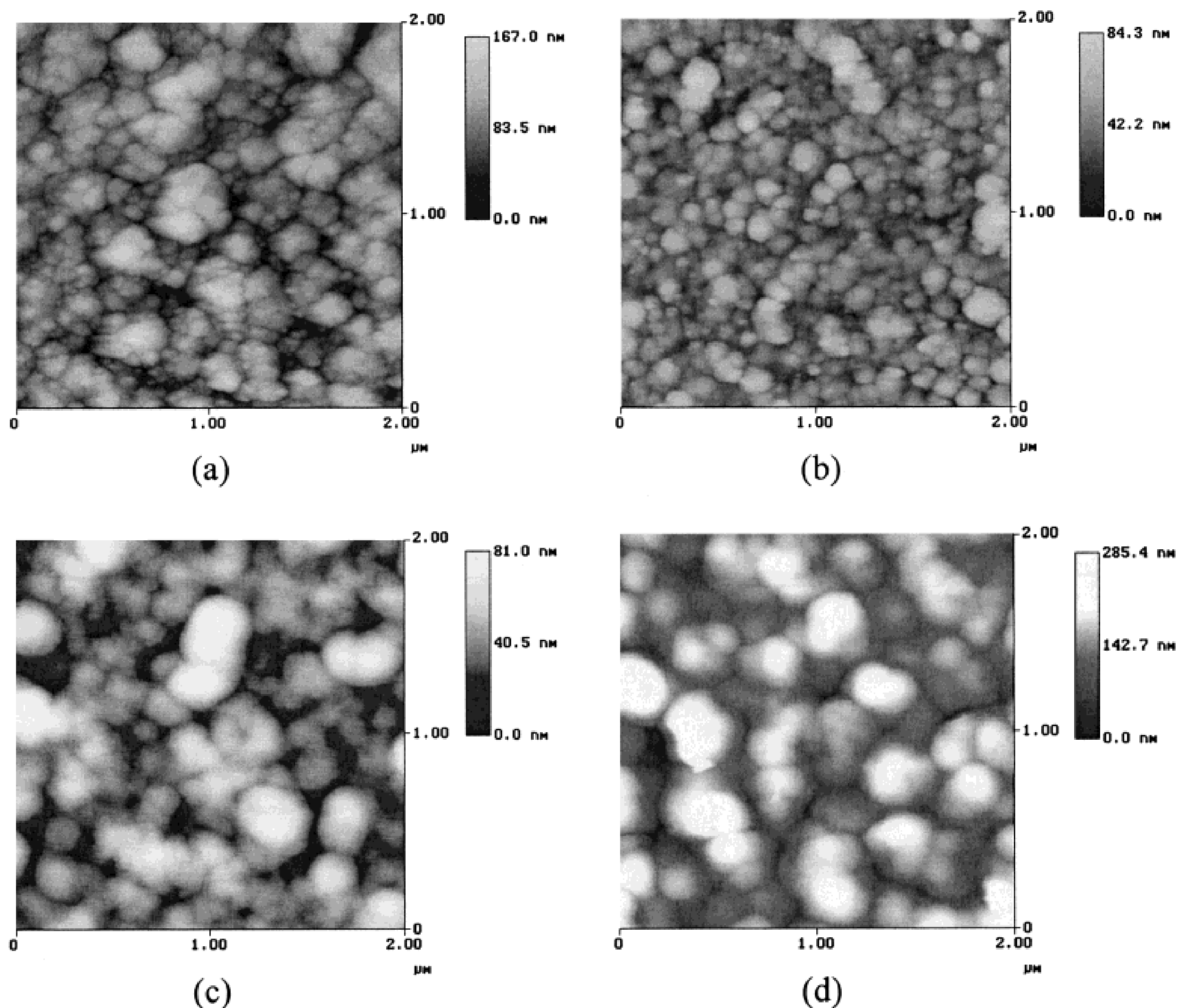

Figure 1 2D AFM surface images of pulsed plasma films deposited from 1,1,2,2-$C_2H_2F_4$, CH_2F_2, and HFPO. All films show nodular growth, with the size and distribution of nodules dependent on the pulse cycling condition and precursor, which in turn determine the energy input to the growing surface per nm of deposited film and the pulsed plasma chemistry. (a) 10/100 $C_2H_2F_4$, (b) 10/100 CH_2F_2, (c) 10/100 HFPO, (d) 10/400 HFPO.

for the film grown from HFPO [Fig. 1(c)] reveals nodules that are significantly larger than those seen in either Figure 1(a) or (b). The nodule diameters in Figure 1(c) range from 130 to 260 nm, and there is also a distribution of nodule heights. Indeed, those taller, larger nodules could be physically blocking the supply of growth species to the lower nodules, otherwise known as shadowing.[19,20] Surprisingly, however, in comparison to the film grown from CH_2F_2, the maximum feature height is slightly lower (81 nm). Also, the corresponding rms roughnesses are similar (12.3 nm).

The shadowing effect observed for the HFPO precursor is even more apparent when a longer pulse off-time is used. Figure 1(d) shows a 2D AFM surface image of a 10/400 pulsed plasma film deposited from HFPO (422 nm thick). The nodules are a bit larger ($d \sim 180$–270 nm) and now the maximum height has jumped to approximately 285 nm. The rms roughness reflects these changes, increasing to 35.6 nm.

In CH_2F_2 pulsed plasmas, HF and free fluorine are the dominant products.[17] These species are also present in lesser concentrations in $C_2H_2F_4$

Table I Deposition Conditions, Film Thickness, Root Mean Square Roughness (R_{rms}), Maximum Feature Height, and Nodule Diameters (d) for Various Films

Precursor	Pulse	Substrate	Film Thickness (nm)	Dep. T (C)	R_{rms} (nm)	Max. Feature Height (nm)	d (nm)
HFPO	10/20	Si	399	25	0.88	11.63	20–40
	10/50	Si	515	25	4.04	44.04	85–150
	10/100	Si	438	25	12.3	80.88	130–260
	10/200	Si	484	25	31.7	217.07	120–190
	10/400	Si	422	25	28.4	285.44	180–270
	10/400	Si	687	60	12.5	80.68	140–250
	10/400	Si	556	110	10.7	65.71	130–200
	10/400	Al/Si	470	25	26.9	171.41	170–260
$C_2H_2F_4$	10/100	Si	516	25	22.3	166.70	20–50
							100–150
	40/400	Si	~ 340	25	41.1	337.62	70–110
	10/100	Al/Si	564	25	21.5	181.66	20–80
	40/400	Al/Si	~ 430	25	67.1	431.06	50–90
CH_2F_2	10/100	Si	364	25	11.8	84.31	30–100
	40/400	Si	770	25	47.8	338.91	60–100
	10/100	Al/Si	356	25	15.2	151.99	30–50
	40/400	Al/Si	~ 540	25	32.8	250.24	40–80

pulsed plasmas, but are absent in HFPO pulsed plasmas. More HF and free fluorine in the plasma correlates to smaller nodule sizes in films produced at the same excitation conditions [e.g., 10/100, Fig. 1(a)–(c)]. This suggests F ions and atoms aid the nucleation of new nodules. However, many variables are coupled in the plasma environment, so it difficult to make definitive statements. In creating HF and free fluorine in the plasma, carbon-rich species must be made and these may also play a role in nucleation. In support of this hypothesis, note that the percentage of unfluorinated carbon in the films decreases with reduced tendency of the precursor to undergo HF elimination.[16,17]

It is known that the CF_x fractions for films grown from HFPO pulsed plasmas are dependent on the absolute pulse on- and off-times.[15] HFPO pulsed plasmas are known to have high concentrations of CF_2 in the gas phase due to the initial decomposition of HFPO into CF_2 + $CFOCF_3$, with those concentrations also dependent on the absolute pulse on- and off-times.[17] For a fixed pulse on-time, the percent CF_2 in the deposited film increases with increasing pulse off-time, whereas other CF_x species decrease, reflecting both the change in the available CF_2 and the decrease in surface modification due to ion bombardment, chemical etching, and other plasma-induced surface damage mechanisms as pulse off-time is increased.[15] These changes in plasma chemistry (i.e., available depositing species) and surface modification likely control the geometry of nodule formation during film growth as well. The degree to which a growing surface will be subjected to surface modification is dependent on both the pulse on-time and the film growth rate. Figure 2(a) plots R_{rms} and the incident power/deposition rate per pulse cycle (J × cycle/nm), Q, as a function of the pulse off-time for a series of films deposited from HFPO (pulse on-time fixed at 10 ms). The incident power is calculated as the peak power (280 W) multiplied by the length of the pulse on-time. Figure 2(a) shows a decrease in Q as pulse off-time increases, whereas R_{rms} increases. Thus, at short off-times the growing surface is subjected to the most modification, leading to smoother surfaces; whereas, as pulse off-time is increased, less modification occurs, resulting in a rougher surface.

The degree of surface modification to which a growing film is subjected also accounts for the decrease in R_{rms} as the substrate temperature during deposition is increased. Figure 2(b) shows R_{rms} and Q as a function of the substrate deposition temperature for a series of 10/400 HFPO pulsed plasma films. As the substrate temperature increases, Q also increases, whereas R_{rms} decreases, indicating that at higher temperatures, the growing film is subjected to increased

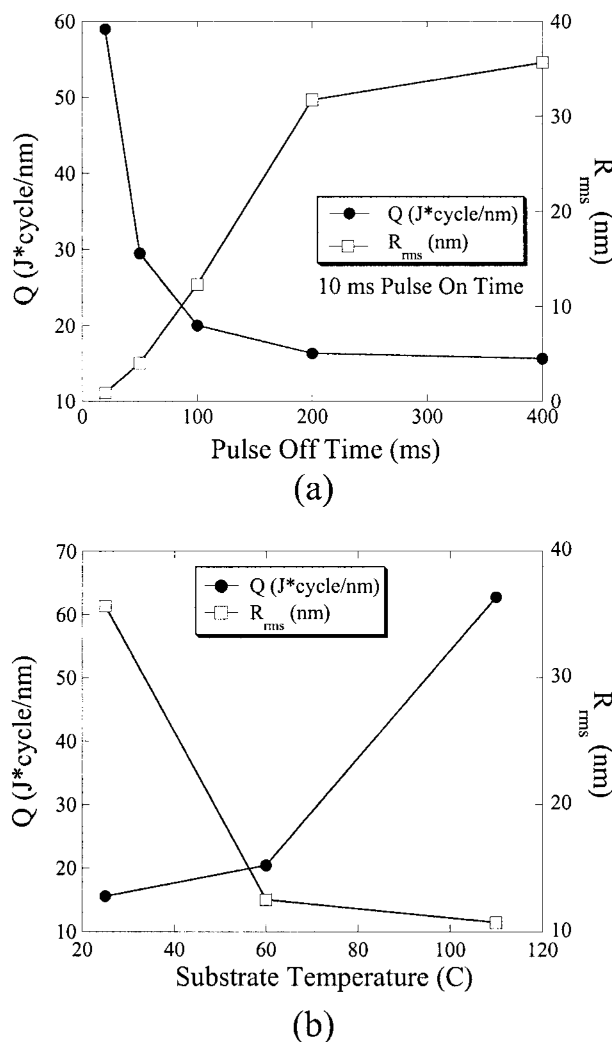

Figure 2 (a) R_{rms} and the incident power/deposition rate per pulse cycle (J × cycle/nm), Q, as a function of the pulse off-time for a series of films deposited from HFPO. At short off-times the growing surface is subjected to the most modification, leading to smoother surfaces. As pulse off -time is increased, less modification occurs, resulting in a rougher surface. (b) R_{rms} and Q as a function of the substrate deposition temperature for a series of 10/400 HFPO pulsed plasma films. Q increases with increasing substrate temperature, whereas R_{rms} decreases, indicating that at higher temperatures, the growing film is subjected to increased modification. The changes in R_{rms} observed here are directly due to the increased surface modification, since the CF_x distribution does not change significantly for these films as substrate temperature is increased.[15]

modification, leading to the decrease in R_{rms}. It is especially important to note that the CF_x distribution does not change significantly for these films as substrate temperature is increased.[15] Therefore, the changes in R_{rms} observed here are directly due to the increased surface modification, as opposed to the data presented in Figure 2(a), where both percent CF_2 and Q increase with pulse off-time.

The results obtained for films deposited from $C_2H_2F_4$ and CH_2F_2 can also be partially explained in terms of surface modification mechanisms. Comparing R_{rms} and Q for 10/100 pulsed plasma films from all three precursors (Table II), R_{rms} is once again inversely related to Q. However, the power factor Q does not account for the jump in R_{rms} when comparing 10/100 and 40/400 films deposited from $C_2H_2F_4$ and CH_2F_2. For $C_2H_2F_4$, Q actually increases, whereas R_{rms} doubles. For CH_2F_2, there is a slight decrease in Q, but this decrease is not sufficient to explain the increase in R_{rms}. Clearly, another mechanism must be in effect. Unfortunately, the data presented here are not sufficient to postulate this additional mechanism.

Figure 3 shows a 2D AFM surface image of a 10/100 pulsed plasma film deposited from CH_2F_2 onto an Al-coated Si substrate (film is 356 nm thick). In comparison with Figure 1(b), in which the film was deposited on a bare Si substrate, it can be seen that the surface morphology has changed as a result of the Al coating. The nodules are generally much smaller ($d \sim 30$–50 nm), but the maximum feature height has almost doubled, to 152 nm. Despite this increase in feature height, due to the smaller distribution of nodule sizes, the rms roughness is only slightly larger (15.2 nm). In general, the nodule sizes were found to decrease for all of the films deposited on the Al-coated Si versus bare Si substrates (all precursors). The maximum feature heights also changed, but they did not all follow the same trend. The rms roughness generally followed the maximum feature height, since those changes were usually larger than the change in nodule size (see Table I). These changes in surface morphology can be traced directly to the surface properties of the substrate. Bare Si is extremely smooth, with R_{rms} = 0.53 nm and a maximum feature height of 9.47 nm. In contrast, the Al-coated Si substrate has clearly distinguished fingerlike structures ($d \sim 60$–100 nm), leading to R_{rms} = 7.48 nm and a maximum feature height of 57.26 nm. These fingerlike structures clearly influence the size and distribution of the fluorocarbon film nodules that grow from them.

It is of interest to make a connection between the surface structures seen here and those ob-

Table II Comparison of R_{rms}, Maximum Feature Height, Nodule Diameter (d), and Incident Power Factor (Q) for 10/100 Films Deposited from all Three Precursors[a]

Precursor	Pulse	Thickness (nm)	Dep. Rate (nm/cycle)	R_{rms} (nm)	Max. Feature Height (nm)	d (nm)	Q (J × cycle/nm)
HFPO	10/100	438	0.14	12.3	80.88	130–260	20.0
$C_2H_2F_4$	10/100	516	0.278	22.3	166.70	20–50 100–150	10.1
	40/400	~ 340	0.593	41.1	337.62	70–110	18.9
CH_2F_2	10/100	364	0.074	11.8	84.31	30–100	37.9
	40/400	770	0.304	47.8	338.91	60–100	36.8

[a] Data for 40/400 films deposited from $C_2H_2F_4$ and CH_2F_2 are also present for comparison with the 10/100 condition.

served in the literature for various types of deposited films. Movchan and Demchishin were the first to propose a generalized structure zone model (SZM), which correlated observed film morphology with a normalized process parameter, in this case T/T_m, where T is the deposition temperature and T_m is the melting point of the deposited film.[19] They identified three different growth regimes based on the observed microstructure of the films. Thornton later added to this model by proposing a transitional region (zone T) between Movchan and Demchishin's zones 1 and 2.[20] According to this model, microstructural development is controlled, in turn, by shadowing effects (zone 1), surface diffusion (zone T and zone 2), and bulk diffusion (zone 3) as T/T_m increases.[19–21] Each zone has particular material properties associated with it, and thus, by identifying the relevant growth zone for a particular material, it was possible to infer some of its material properties. It is important to note that these studies were based on both evaporated and sputtered metals and metal oxides.[19,20] Hence, it cannot be automatically assumed that covalently bonded PECVD films would necessarily conform to the SZM. However, several covalently bonded systems have been studied, and the SZM has been successfully applied to these systems.[18] All of the films investigated here were found to be zone 1 growth structures. This categorization is evident from the AFM images in Figures 1 and 3, and can also be seen clearly in Figure 4, which shows a SEM micrograph of a 10/50 pulsed plasma film from HFPO deposited over a polysilicon resistor structure. The nodules observed with the AFM are clearly seen in the open areas, as well as columnar growths over the device structures. The ability to smooth the film microstructure by increased plasma exposure suggests this energy input to the surface promotes atomic rearrangements, analogous to the manner in which increasing temperature allows for increased surface and bulk diffusion. Thus, the dominance of a shadowing effect proposed earlier for the films from HFPO is confirmed with the identification of these films (as well as those from $C_2H_2F_4$ and CH_2F_2) as zone 1 growth structures.

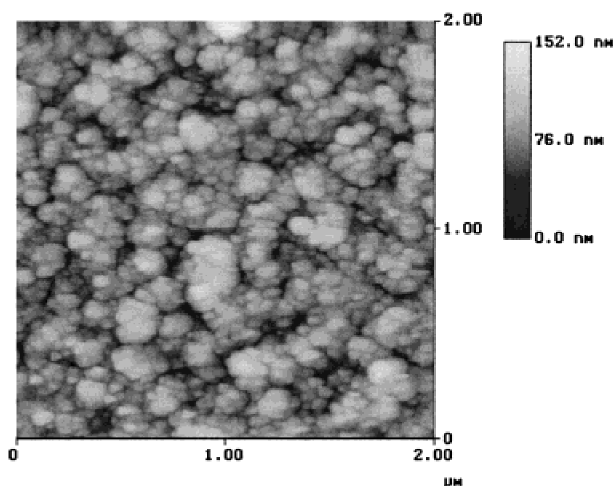

Figure 3 2D AFM surface image of 10/100 CH_2F_2 pulsed plasma film deposited on an Al-coated Si substrate. In comparison with Figure 1(b), the nodule diameter has decreased, whereas the maximum feature height has almost doubled. Despite the increase in maximum feature height, due to the smaller nodule size distribution, R_{rms} is not significantly changed from the sample deposited on bare Si (15.2 versus 11.8 nm).

All of the advancing contact angles measured for pulsed plasma films from HFPO, as well as those from $C_2H_2F_4$ and CH_2F_2, are well above 90°. A contact angle $> 90°$ indicates a nonwetting surface, whereas one $< 90°$ is indicative of a wetting surface.[22] For reference, the advancing con-

tact angle for polytetrafluoroethylene (PTFE) is approximately 108°.[22] Measured contact angles can be affected by a film's surface roughness, fluorine-to-carbon ratio, and degree of oxidation.[3,4,22] Oxidation occurs through the formation of C═O, OH, and COOH groups by reaction of dangling bonds formed during the pulsed plasma deposition with ambient water and oxygen.[4] It is assumed for all of these measurements that the differences in degrees of oxidation between samples do not significantly affect the observed contact angles.

All of the HFPO pulsed plasma films were found to have contact angles between 105 and 130°; 10/100 pulsed plasma films from $C_2H_2F_4$ and CH_2F_2 had contact angles of 107 and 101°, respectively, whereas their 40/400 films had contact angles of 144° each. The large increase in contact angles between these two pulse conditions is most likely a function of the increased roughening of the surface at the 40 ms on-time. AFM measurements show that R_{rms} at least doubles between these pulse conditions for both precursors (see Table I).

Figure 5 shows the advancing contact angle for a drop of water on a series of pulsed plasma films, all deposited from HFPO, as a function of the pulse off-time (pulse on-time = 10 ms). Figure 5 highlights two aspects of the HFPO pulsed plasma films. First, there is a general increase in contact angle with pulse off-time. This increase can be attributed to two effects: composition and surface roughness. First, it is known that the percent CF_2 in the deposited films increases with pulse off-time.[15] It is also known that CF_x groups are increasingly hydrophobic as $x = 1 \rightarrow 3$.[22] The composition of these films tends to decrease CF and C̲–CF groups while increasing CF_2, with only minor variations in percent CF_3 as pulse off-time is increased.[15] Therefore, an increase in the percent CF_2 for these films should indicate an increasingly hydrophobic environment, which would result in a higher contact angle. Most of the contact angles observed here are slightly over 108°, the contact angle for water on PTFE. Since PTFE presents a CF_2-only surface, it can be as-

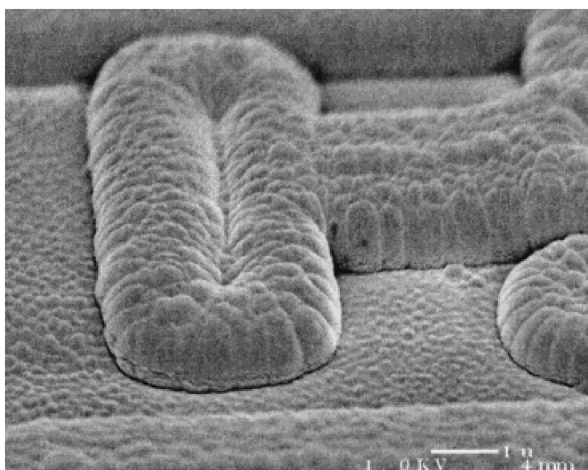

Figure 4 SEM micrograph of a 10/50 HFPO pulsed plasma film deposited over a polysilicon resistor structure. The nodules observed with the AFM are clearly seen in the open areas, as well as columnar growths over the device structures. The observed surface morphology emphasizes the zone 1 nature of the deposited film.

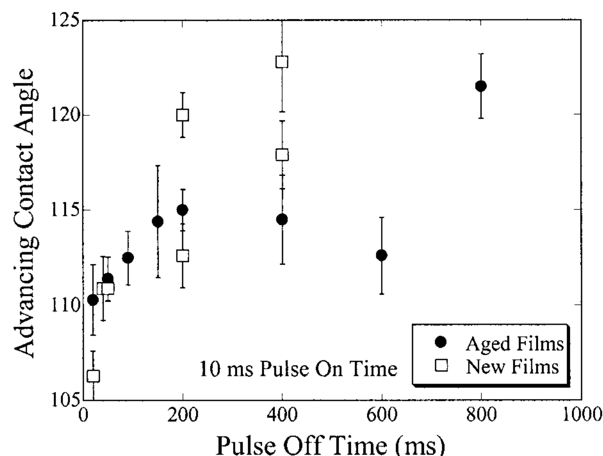

Figure 5 Advancing contact angle for a drop of water on a series of HFPO pulsed plasma films as a function of the pulse off-time (pulse on-time = 10 ms). Two aspects of the HFPO pulsed plasma films are highlighted. First, there is a general increase in contact angle with pulse off-time, which can be attributed to two effects: change in CF_x composition and increased surface roughness. For this series of films, percent CF_2 generally increases with pulse off-time, whereas percent CF_3 stays relatively the same. The increase in percent CF_2 will lead to an increase in hydrophobicity, contributing to the increase in contact angles. Second, freshly grown films deposited at longer pulse off-times have higher contact angles than their aged counterparts, whereas those at short off-times have similar or smaller contact angles. These types of trends have been seen in other PECVD fluorocarbon systems and were expected, since general handling of the older films would result in contamination and alteration of the surface oxidation of free radicals and unsaturated carbon bonds after plasma deposition can also contribute to a decrease in contact angle.

sumed that the approximately 15% CF_3 also present in these films contributes to the higher contact angles. The second contribution to the increasing contact angles can be traced to the increase in surface roughness as pulse off-time is increased [Fig. 2(a)]. Roughness is known to increase any observed contact angles,[4,22] and therefore since R_{rms} increases with pulse off-time for these films, an increase in contact angle is also expected.

The second trend that Figure 5 emphasizes is that freshly deposited films (contact angles measured within 2 days of deposition) can give results that are different from those for films aged for several months (>6 months). In general, newly grown films deposited at longer pulse off-times have higher contact angles than their aged counterparts, whereas those at short off-times have similar or smaller contact angles. These types of trends have been seen in other PECVD fluorocarbon systems[23] and were expected since general handling of the older films would result in contamination and alteration of the surface. Oxidation of free radicals and unsaturated carbon bonds after plasma deposition has also been seen widely in the literature.[3,4] The introduction of C=O groups into the films increases the surface energy of the plasma polymer, resulting in a decrease in the contact angle.[4,22,24] This mechanism most likely also plays a role in the long pulse off-time trend seen here.

Significant hysteresis was also observed for all of the pulsed plasma films measured, with retreating contact angles generally 89–92°. The trends observed with the advancing contact angle do not translate to the retreating angle, as the retreating contact angles are less susceptible to effects such as roughness.[4]

CONCLUSIONS

AFM measurements have been made on a series of fluorocarbon films deposited from pulsed plasmas of HFPO, 1,1,2,2-$C_2H_2F_4$, and CH_2F_2. All of the films give images showing nodular growth (cauliflower-like appearance), with the size and distribution of the nodules dependent on both the precursor, the degree of surface modification to which the growing film is exposed, and the substrate surface. Films deposited from $C_2H_2F_4$ showed clusters of smaller nodules around larger nodules, whereas films deposited from CH_2F_2 were characterized by a uniform distribution of smaller nodules, and films deposited from HFPO had the largest observed nodules. For films deposited from HFPO, it was found that the rms roughness increased with increasing pulse off-time, whereas for a fixed pulse condition, the roughness decreased with increasing substrate temperature. These changes can be partially attributed to the change in incident power per nm of film deposited as either pulse off-time or substrate temperature is varied. Films from all of the precursors were also sensitive to the surface structure of the deposition substrate, with the rougher Al-coated Si surface affecting both the nodule size and distribution for all of the deposited films. Movchan and Demchishin's structure zone model was applied to the observed films, which were all found to be zone 1 structures, indicating that film growth is dominated by shadowing effects. Advancing contact angles for all of the films were found to be higher than that of PTFE (108°), indicating both hydrophobic and rough surfaces. Specifically, contact angles of films deposited from HFPO were found to increase with pulse off-time, the same trend observed for both the CF_2 fraction of the film and the rms roughness.

The authors gratefully acknowledge the financial support of the Office of Naval Research, Lucent Technologies Bell Laboratories Graduate Research Program for Women, and the NSF/SRC Engineering Research Center for Environmentally Benign Semiconductor Manufacturing. We also thank DuPont for donation of the feed gases used in this study, and Emily Sung for her work with the contact angle measurements.

REFERENCES

1. Endo, K. MRS Bull 1997, 22(10), 55.
2. Endo, K.; Tatsumi, T. Appl Phys Lett 1996, 68(20), 2864.
3. Yasuda, H. Plasma Polymerization; Academic Press: New York, 1985.
4. d'Agostino, R. Ed. Plasma Deposition, Treatment, and Etching of Polymers ; Academic Press: Boston, 1990.
5. Hopkins, J.; Boyd, R. D.; Badyal, J. P. S. J Phys Chem 1996, 100(16), 6755.
6. Miller, J. D.; Veeramasuneni, S.; Drelich, J.; Yalamanchili, M. R.; Yamauchi, G. Polym Eng Sci 1996, 36(14), 1849.
7. Jou, J.-H.; Cheng, C.-L.; Jou, E. C.-Y.; Yang, A. C.-M. J Polym Sci B Polym Phys 1996, 34, 2239.
8. Beamson, G.; Clark, D. T.; Deegan, D. E.; Hayes, N. W.; Law, D. S.-L.; Rasmusson, J. R.; Salaneck, W. R. Surf Interface Anal 1996, 24, 204.
9. Dietz, P.; Hansma, K.; Ihn, K. J.; Motamedi, F.; Smith, P. J Mater Sci 1993, 28, 1372.

10. Hansma, H.; Motamedi, F.; Smith, P.; Hansma, P.; Wittman, J. C. Polymer 1992, 33(3), 647.
11. Coen, M. C.; Dietler, G.; Kasas, S.; Groning, P. Appl Surf Sci 1996, 103, 27.
12. Nysten, B.; Roux, R.-C.; Flandrois, S.; Daulan, C.; Saadaoui, H. Phys Rev B Solid State 1993, 48(17), 12527.
13. Hopkins, J.; Badyal, J. P. S. J Polym Sci A Polym Chem 1996, 34, 1385.
14. Magonov, S. N.; Whangbo, M.-H. Surface Analysis with STM and AFM; VCH, New York, 1996.
15. Limb, S. J.; Edell, D. J.; Gleason, E. F.; Gleason, K. K. J Appl Polym Sci 1998, 67, 1489.
16. Labelle, C. B.; Gleason, K. K. J Vac Sci Technol A 1999, 17(2), 445.
17. Labelle, C. B.; Karecki, S.; Reif, R.; Gleason, K. K. J Vac Sci Technol A, to appear.
18. Messier, R.; Yehoda, J. E. J Appl Phys 1985, 58(10), 3739.
19. Movchan, B. A.; Demchishin, A. V. Phys Met Metallogr 1969, 28, 83.
20. Thornton, J. A. Annu Rev Mater Sci 1977, 7, 239.
21. Messier, R.; Giri, A. P.; Roy, R. A. J Vac Sci Technol A 1984, 2(2), 500.
22. Adamson, A. W. Physical Chemistry of Surfaces, 5th ed.; Wiley: New York, 1990.
23. Gengenbach, T. A.; Griesser, H. J. Surf Interface Anal 1998, 26, 498.
24. Johnston, E. E.; Ratner, B. D. J Electron Spectrosc Relat Phenom 1996, 81, 303.